3D Characterisation of Microporosity in Carbonate Cores

Abid Ghous[1,2], Tim J. Senden[1], Rob M. Sok[1], Adrian P. Sheppard[1], Val W. Pinczewski[2] and Mark A. Knackstedt[1,2,*]
[1]Department of Applied Mathematics, Research School of Physical Sciences and Engineering, Australian National University, Canberra, Australia,0200
[2]School of Petroleum Engineering, University of New South Wales, Sydney, Australia
* Corresponding Author: mark.knackstedt@anu.edu.au

This paper was prepared for presentation at the SPWLA Middle East Regional Symposium held in Abu Dhabi, April 15-19, 2007.

ABSTRACT

Carbonates, accounting for majority of oil and gas reservoirs, are well known for their broad, but complex, pore size distribution and pore geometries. Generally the heterogeneiety of carbonates is dominated by submicron porosity. This substantially affects log measurements of petrophysical properties resulting in erroneous reserve estimation, production and recovery rates. This feature of carbonates strongly encourages the topological and morphological pore scale characterisation at the submicron level. In this paper, we use micro Computed Tomography(μCT) and Focussed Ion Beam (FIB) microscopy to describe 3D imaging of microporosity in carbonate core samples. Micro-CT is capable of acquiring 3D images of individual cores at the macropore level down to resolutions of a few microns. However, a great limitation is that it cannot directly access microporous regions. For those regions we use Focussed Ion Beam microscopy to mill and an electron beam to image the exposed surface at a resolution down to few nanometres. FIB is employed to study the general structure of the microporosity and in particular its connectivity. This generalised structural information is then related back to the sub-resolution microporosity in the μCT. By combining μCT and FIB one can undertake a study of permeability and resistivity of core material incorporating both the macroporosity and microporosity over many length scales.

INTRODUCTION

Carbonate formations are considered extremely complex when estimating oil and gas production due to their inconsistent correlation between porosity and permeability. The presence of irregularly shaped pores of various sizes makes the assignment of a consistent relationship nearly inconcievable. Traditionally, reservoir engineers and petrophysicists develop a relationship based on the pore size and structure of a given interval of a reservoir to predict the fluid flow. This is achieved by defining porosity based on pore types and pore size distribution e.g vuggy porosity, macroporosity, microporosity and then characterising it for flow properties. Presence of abundant microporosity, observed in many carbonates, severely affects any such attempt. The distribution of microporosity plays a central role in formation evaluation, understanding of production rates and overall field performance. However, as pervasive as this component is, it is constituted of sub-micron structure and thus very difficult to describe at a pore-scale.

The connectivity of macropores and the partitioning of liquid phases are inherently three dimensional problems and microtomography is a valuable tool in understanding how microporous regions relate these properties to multiphase flow. Two goals are desirable in describing microporosity: the connectivity of all porosity, particularly where micro- connects macroporosity, and quantification of local porosity and permeability. As with any imaging technique it becomes difficult to make purely structural interpretations when relevant structures are beyond the resolving power of a technique. In conventional microtomography several microns resolution is readily attainable, however microporosity requires resolution well below to tens of nanometres. This is confounded by the large range of length scales. A single technique alone could not hope to resolve the smallest pore while describing a large enough volume to be useful. Clearly, direct structural elucidation is unfruitful and a different approach to determining pore connectivity needs to be made. X-ray tomography has the opportunity to offer interpretation below these resolution limits by relating a partial volume to an assumed porosity. Presented here is an approach to relate effective volumes to the material density maps provided by tomography as input into computer models. To aid this relationship and better understand two and three phase flow properties, it will be necessary to determine a realistic pore-scale description. While μCT offers a generic multi sample analysis, FIB microscopy offers a limited view at the micropore scale for a select range of samples. In this way FIB data is

used to generalise permeability for microporous regions identified in μCT data. As an ensemble, this total pore description feeds into computer models. The connectivity of pore spaces is also crucial for determining resistivity indices and exponents as a function of saturation and hence better interpretation of logging measurements.

Using a purpose built μCT we image small subsets of carbonate reservoir cores at $\sim$ 3 micron(voxel) resolution. The resultant images yield 3D density maps of the sample. These are binarised to differentiate 3D structure of pores above this voxel resolution by applying a technique, called 3-Phase Segmentation. In this process density values are divided into solid, pores or micropores, the later two partitions being summed to determine effective porosity values. However, this method may lack certainity in two important ways. Firstly, the connectivity of pores, whether or not there is a connection present between macropores and micropores may be over interpreted. Secondly, inaccuracies in phase partioning mean a region assigned as micropore might instead be a mineral with lower average density. These uncertainities can be overcome to some extent by saturating the sample with an X-ray opaque liquid and then again imaging giving a more certain partitioning of micropores. This method complements the porosity calculation based on attenuation values. 3D visualisation is used as a useful tool to study the structure and connection between different porosities in a quantitative way. Network representations of the microporosity and macroporosity give an indicative spatial representation of the pore coupling.

3D Tomographic Imaging

The high-resolution and large-field X-ray μCT facility used here to analyse the 3D pore structure of core plugs from carbonate reservoirs was developed in-house (Arns et al., 2005; Sakellariou et al., 2003). The X-ray source produces a polychromatic X-ray beam and the projection data is collected using a cone beam along a circular trajectory. The conventional experimental preparation for analysis involves coring a $3-5\ mm^2$ diameter sub-plug from a fragment of the plug provided. Imaging is then undertaken on this sub-plug at 2000^3 with a voxel resolution of $2-3\ \mu m$. The data is then reconstructed to give a 3D density map of the imaged sample. Fig. 1 shows the example of greyscale images of a coronal slice through the middle of a typical clastic and one of the carbonate samples studied here. The carbonate is an intraclastic-peloidal grainstone with a porosity of 29.8%. It has 1010 mD air permeability and $2.71 g/cm^3$ grain density details of this formation can be found in (Masalmeh and Jing, 2004).

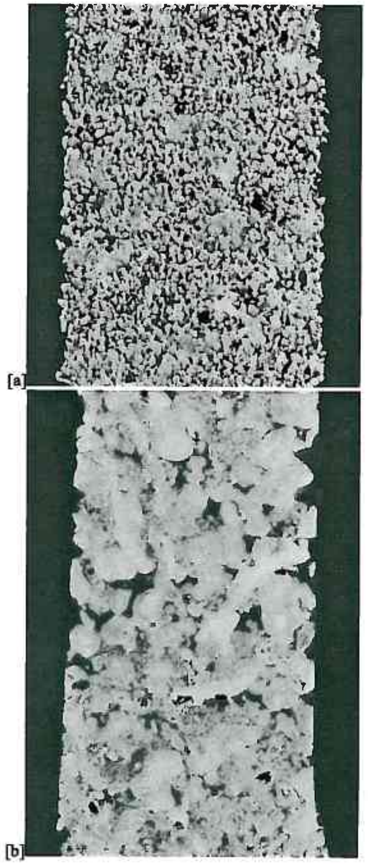

Figure 1: Greyscale coronal slice of a 5mm diameter clastic sample(a) and a carbonate sample(b) tomograms.

Quantification of Microporosity

Tomographic images consist of a cubic array of linear X-ray attenuation coefficient values each corresponding to a voxel of the sample. To undertake any analysis, data needs to be partitioned into regions of pore and solid. This process of partioning into disjoint regions is known as segmentation and involves a nontrivial local neighbourhood decision for each voxel. Ideally one would wish to have a multi-modal distribution of attenuation coefficients giving unambiguous phase separation. Unfortunately, the presence of low density pore inclusions (microporosity) as insufficient edge resolution leads to a spread in the low density signal making it difficult to *unambiguously* differentiate the pore from the microporous and solid mineral phases as shown in Fig. 2.

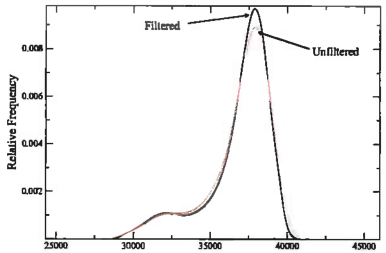

Figure 2: Intensity histograms of unfiltered and filtered datasets from carbonate sample shown in Fig. 1(b).

In carbonates, microporosity induces a broad intensity distribution accounting for a lower density signal. Here we present a technique where the microporosity is segmented along with the usual partioning of solid and pore phases. It requires a 3 Phase segmentaion where one phase belongs to partially filled voxels, or potential microporosity. A small subset, 500 x 800 x 1700 voxels, was chosen out of imaged sample for processing. The subset was first filtered with an anisotropic diffusion filter which removes the noise while preserving the important edge features. The parameters for the three phase segmentation were:

T_1	32500
T_2	34500
T_3	36500
T_4	38500
G_1	1800
G_2	4300

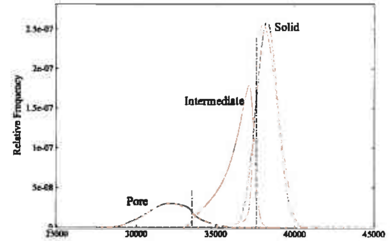

Figure 3: *Resultant Intensity histogram. The solid lines show the resultant histograms of the three phases after segmentation. The dashed curves show the gaussian fits of the pore and the solid phase. The dotted-dashed vertical lines show the mean plus (and minus) standard deviation of the gaussian fits.*

T stands for different thresholds and G for Gradients; their details can be found in (Sheppard et al., 2004). The assignment is as follows: for every voxel we have an intensity value I_n and a local intensity gradient value g_n. Now if

$I_n < T_1$ and $g_n < G_2$ voxel is *pore phase*
$I_n > T_4$ and $g_n < G_2$ voxel is *solid phase*
$T_2 \leq I_n < T_3$ and $g_n < G_1$ voxel is *intermediate phase*

The phase of all unassigned voxels is then determined through our active contour growing algorithm. The images of resulting phases after segmentation are shown in Fig. 4 and intensity distributions of the resulting phase assignments is indicated in Fig. 3. In this method, we performed a gaussian fit (dashed lines in Fig. 3) to both the pore (subscript p) and the solid phase (subscript r) and determined the mean ($\overline{I}_{phase}$) and standard deviation (σ_{phase}) of the distributions. For the assignment of the microporosity we analysed the intermediate phase. To any voxel n in the intermediate phase that has an intensity value I_n less than: $\overline{I}_p + \sigma_p$ we assign 100% porosity. To any voxel in the intermediate phase with I_n larger or equal than: $\overline{I}_r$ - σ_r we assign 0% porosity. Any voxel with I_n in between these two cutoff intensities, we assign a linearly scaled microporosity value m_n:

$$m_n = \frac{((\overline{I}_r - \sigma_r) - I_n)}{(\overline{I}_r - \sigma_r) - (\overline{I}_p + \sigma_p)} \quad (1)$$

And the total porosity ϕ is then calculated as

$$\phi = \frac{N_p + \sum_{n=0}^{N_i} m_n}{N_{tot}} 100\% \quad (2)$$

Where N_p is the number of voxels in the pore phase, N_i

the number of voxels in the intermediate phase, and N_{tot} is the total number of voxels in the sample. The resulting fractions of phases were: N_p/N_{tot} = 12.2%, N_i/N_{tot} = 36.8% and N_r/N_{tot} = 51%. The total porosity using this method is calculated as 27.5% with 15.3% being assigned to microporosity. This matches rather favourably with the experimental porosity and with MICP curve for microporosity of the intraclastic-peloidal grainstone shown in (Masalmeh and Jing, 2004).

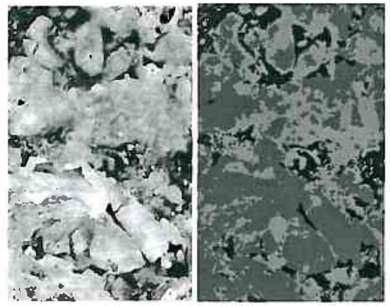

Figure 4: Left: Zoomed view of original Image, Right: segmented showing macro(black), micro(light grey) and solid(dark grey) region.

To visualise the microporosity we divided the intermediate phase into four regions of 25% each and assigned each voxel within the intermediate phase to one of the four regions. Fig. 5 shows individual mapping of all 4 microporosity regions onto the greyscale image. In Fig. 6 we can see delineation of microporosity on full slice in the sample axis. A subset of 700 x 600 is zoomed alongwith greyscale section to visualise microporosity more clearly in Figure 7.

Visually and spatially this technique is found to correlate well with expected distributions of porosity. However porosity quantification is not the sole purpose of the exercise. An important parameter is pore connectivity, a feature which remains somewhat ambiguous for analysis of the dry pore space alone. We next discuss another method to characterise the connectivity of micropores by first imaging the sample dry at a slightly lower resolution then imaging saturated completely with an X-ray opaque liquid. We then take a difference map of both tomograms which gives an intermediate map delineating microporous regions. This approach sheds light on which partial volumes constitute continuously connected porosity.

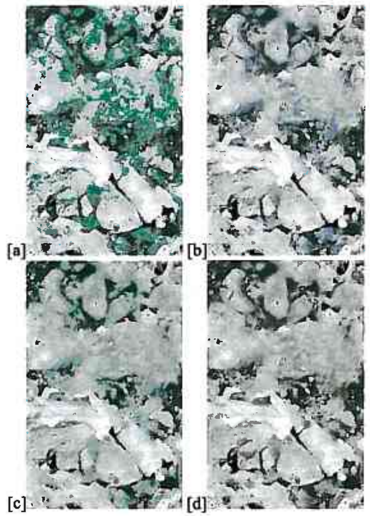

Figure 5: Slices showing regions of different microporosity along Z direction [a] 0 - 25 % [b] 25 - 50 % [c] 50 - 75 % [d] 75 - 100 %.

In order to take a difference map of dry and saturated samples, one has to be extremely careful during experiments to prevent movement of the sample. Even a single voxel shift can have serious consequences in determining partial volumes. A cell was built which holds the sample rigidly throughout the series of experiments preventing any detectable movement. A schematic of the cell is shown in Fig. 8. A 50 mm long and 5.2 mm diameter aluminium cylinder is the core of the cell. The bottom of cell is screwed tightly in the center of the rotation stage of CT instrument which allows free rotation of stage without moving the cell. The top of the cell is used for fluid injection and vacuum connections. The sample is attached to a thin aluminium cylinder, the sample carrier, and inserted into the cell. The carrier is compressed with a spring from the top. The spring is fixed into a cavity drilled along the inner-side of the cell stem and stops movement of sample carrier and the sample in any direction during fluid exchange. A carbonate sample of 5mm diameter was cored and inserted into cell by the above mentioned procedure.

An oven dried carbonate sample from another reservoir was first imaged at a voxel resolution of 8 micron. The

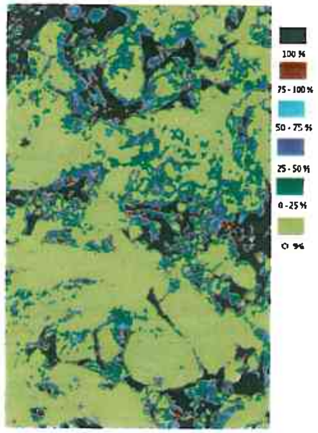

Figure 6: Z-slice showing all microporosity regions mapped onto segmented slice through different colour schemes.

porosity for this carbonate sample was 26.5 %. Carbonates are heterogeneous in regard to their composition, and an attenuation value of lower density solid mineral might be misrepresented as a microporous region. To reduce this ambiguity, a 1.5 mm solid piece of calcite was attached to the top of the sample. This provides a standard reference for zero-porosity pure calcite during the experiment. To choose a liquid for saturation of the sample,different compositions of bromide and iodide solutions were tested for X-ray opacity. A mixture of di-iodomethane (CH_2I_2) and toluene made 50 : 50 (by volume) was considered best for this purpose. Polychromatic X-rays cause non-linearities in the attenuation values and require filtering to avoid any beam hardening effects. A 1 mm thick platinum filter was successfully used to eliminate beam hardening in this case.

It is very important during imaging of saturated core to differentiate between low density mineral and microporous region. Therefore data is referenced by attenuation values of air and normalised by attenuation values of calcite. This normalisation assists in finding a reference point for pore and solid intensity value. As a standard procedure, we took 35 x 35 x 100 cubic voxles subset of the air surrounding the sample and 25 x 25 x 40 cubic voxels from the calcite. A 175 x 175 x 350 cubic voxel subset (shown in Fig. 9) was taken from the original sample. The intensity distributions of all three subsets from both dry and saturated samples are shown in Fig. 10. For

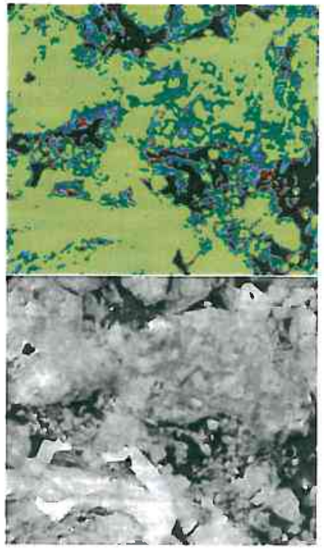

Figure 7: Zooming in on a Z-slice of original and processed subsets to clearly identify microporous regions. size: 700 x 600.

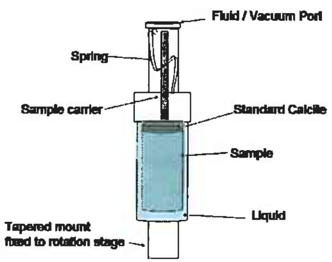

Figure 8: A schematic of cell used to saturate the sample.

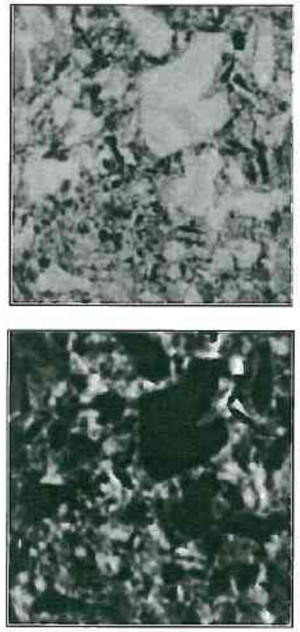

Figure 9: Apparent density map of dry(top) and opaque liquid saturated(bottom) subsets of carbonate sample. In the top dataset, Black denotes a dry macropore while white denotes solid. In the bottom dataset, white denotes saturated macropores and black denotes solid, nonporous phases.

each voxel, the scaled intensity values after normalising with reference air and solid intensities are achieved by:

$$I_{ds} = \frac{(I_{dry} - (\overline{I}_{ad} + \sigma_{ad}))}{(\overline{I}_{cd} - \sigma_{cd}) - (\overline{I}_{ad} + \sigma_{ad})} \quad (3)$$

and

$$I_{ws} = \frac{(I_{wet} - (\overline{I}_{aw} + \sigma_{aw}))}{(\overline{I}_{cw} + \sigma_{cw}) - (\overline{I}_{aw} + \sigma_{aw})} \quad (4)$$

Where I_{ds} and I_{ws} represent scaled intensity values of dry and saturated(wet) datasets respectively. Subscripts d, w, a and c represent dry, wet, air and calcite datasets and $\overline{I}$ and σ are mean and standard deviation of the distributions. The scaled intensity distributions of both subsets are given in Fig. 11. We then subtract both datasets to get the intensity difference of each voxel. The difference plot is shown in Fig. 12 where value of zero represents zero porosity referenced to the calcite standard. We then divide the difference map into three regions; intensity values of zero or less are defined as solid, intensity values of 1 or larger are defined as macropores and intensity values between these two limits are defined intermediate or microporous regions. The representation of these assignments is shown in Fig. 13 where microporosity is shown in greyscale, solid in light blue and macropores in red.

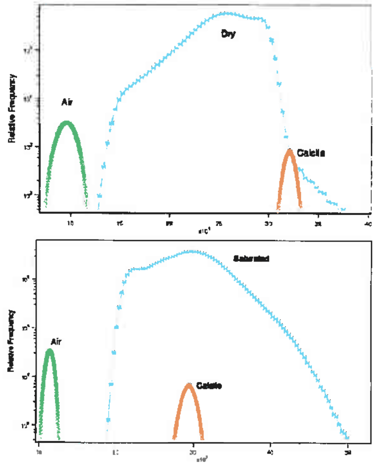

Figure 10: Original intensity histograms, calcite subset and air subset before normalisation. Green curve is air , maroon is calcite and blue is sample subset.

This microporosity evaluation method relies on the linearity of the attenuation values in the intermediate phase(Fig. 12) . All voxels in the microporous region are divided into regions of equal width assigning each region microporosity range of 10%, 20%,......90%. Microporosity contribution of each region is then calculated as :

$$\phi_{ri} = \frac{r_i / \sum_{i=1}^{n} r_i}{f_i} \quad (5)$$

Where $f_i = 10/i$. The microporosity of the dataset is given as:

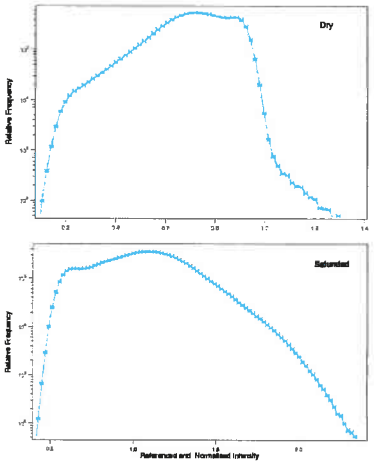

Figure 11: Scaled attenuation distribution obtained after treatment with scaling factor obatined from air referencing and calcite normalisation.

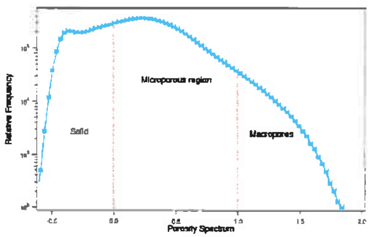

Figure 12: Plot of difference of attenuation values(porosity) of Dry and saturated after scaling. Dotted lines show the limits of microporous region.

$$\phi_{micro} = \frac{N_i}{N_{tot}} \cdot \sum_{i=1}^{n} \phi_{ri} \quad (6)$$

the total porosity ϕ_t is then calculated as:

$$\phi_t = \phi_{macro} + \phi_{micro} \quad (7)$$

The resulting fractions of phases were: N_{macro}/N_{tot} = 2.5%, N_{micro}/N_{tot} = 67.5% and N_{solid}/N_{tot} = 30%.

The porosity using this method is calculated as 27.7% with 25.2% microporosity and compares favourably with experimental porosity. For the particular sample and imaged resolution, most of porosity is counted as microporosity. If experiments are done at higher resolutions, the macroporosity contribution increases while decreasing the microporosity values.

Topology of Microporous Regions

In addition to quantification of microporosity, the connectivity and topology of these micropores remains an important factor in understanding petrophysical properties. Saturation with an opaque liquid also helps in 3D visualization of connected macro- or micropores as we delineate the 3D microporosity distribution and observe its effects on connectivity of pores within a reservoir core. Fig. 14 shows 3D visualisation of the sample imaged with the opaque liquid saturation technique. Fig. 14(a) shows only macropores and one can clearly see most are disconnected at this resolution. We then map the microporous regions onto macropores to see whether or not they connect through micropores as shown in Fig. 14(b). Fig. 14(c) shows a 150 cubic voxel subset of the sample representing all three phases: macropores as green,microporous region as light blue and solid as red.

Pore Network Models

Networks are considered as pore scale reservoir models and can give us quantitative and visual description of pore space and its connectivity. Details of how network models are generated can be found in (Sheppard et al., 2005). Here we present the images of a network generated from the saturated carbonate sample used in saturation imaging (Fig. 9). In Fig. 15(a) we show 175 x 175 x 350 network image of macroporosity, one can clearly see the lack of connectivity in macropores(blue). We then map saturation delineated microporous regions onto macropore network(green) and notice a connection between macro- and micropores. Fig. 15(c) is a 100 cubic voxel network image showing all three phases where red is solid. We also present the plot for one important parameter, coordination number, obtained from network models representing the connectivity of pores. Fig. 16 is a plot of coordination numbers for macro- and micropores. We obtain a volume weighted mean coordination number of 0.73 for macropores and 15.1 for micropores which confirms the degree of connectivity for both phases.

SPWLA Middle East Regional Symposium, April 15-19, 2007

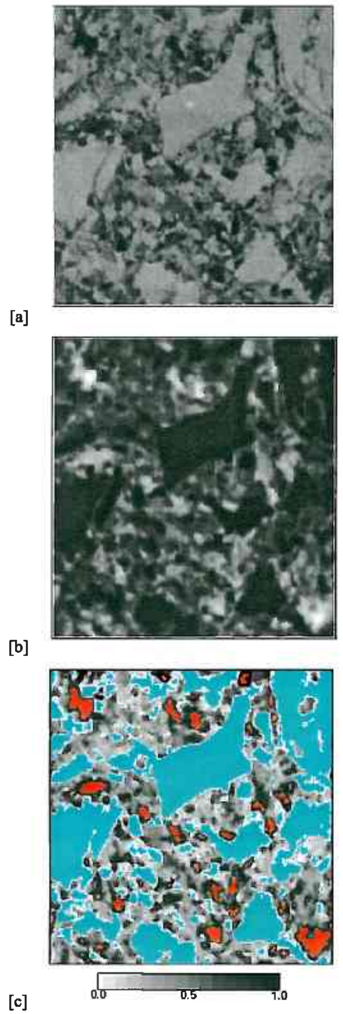

Figure 13: Microporous region comparison of dry, saturated and difference maps of sample used in saturation imaging. (a) Dry image, black is macropore. (b) Saturated image, black is solid and white is macropore. (c) Difference map: blue is solid, red is macropore and microporous region is shown in grey colour with scalebar.

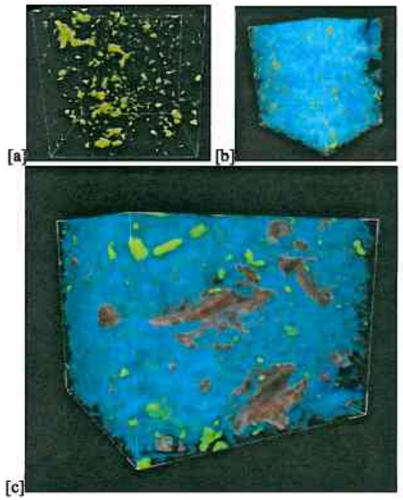

Figure 14: 3D Visulisation of Topology of carbonate core sample used in saturation imaging.[a] pore only [b] pore and microporous phase,showing how they are connected.[c] an enlargement of a 150 cube subset showing all 3 phases.

Pore Structure of Micropores

Network modelling illustrates also pore connectivty but fluid flow and recovery prediction requires structural information as model input. We have shown topology and network models of carbonates but they only show connectivity, and pore structure information at a pore scale higher than the resolution of imaging, i.e. macropores only. To achieve stuructural description of micropores and grains associated with them, we use an advanced microscopy technique called, Focussed Ion Beam microscopy. A Scanning Electron Microscope collects 2D slices of sample while high energy Gallium Ion beam mills the surface away, exposing a fresh surface with each etch. The electron micrographs can be regarded as slices and can be stacked up to make a 3D volume. Although laborious compared with tomography, this information can be a valuable tool to justify any structural choice of network model to simulate fluid flow and residual saturations. We show here the preliminary data to explain how one can view the structure of pores and grains using focussed ion beam. Fig. 17 show series of 3.5 x 3.5 micron slices taken out of the carbonate sample used

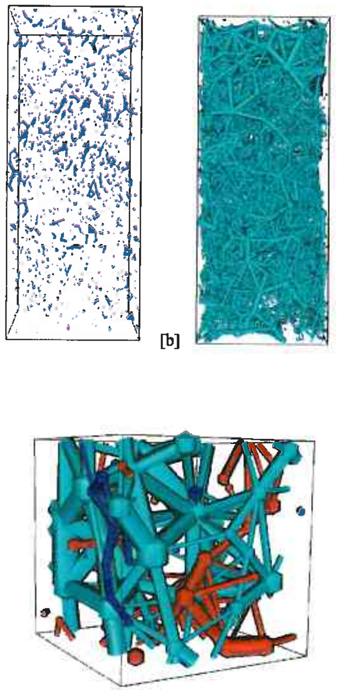

[a] [b]

[c]

Figure 15: 3D pore throat network models of carbonate sample used in saturation imaging (size: 175 x 175 x 350). (a) macropores only network model; note disconnected macropores. (b) after decorating with micropores. (c) zoomed in on a 100 cube subset showing solid region along with macro- and micropores.

earlier in 3-Phase Segmentation technique at a resolution of around 3 nanometre. Successive slices are 200 nm apart. Further processing will involve image registration and segmentation before these 3D volumes can be included in any simulation. This work is currently being undertaken and will be used as input to network models which incorporate microporous information.

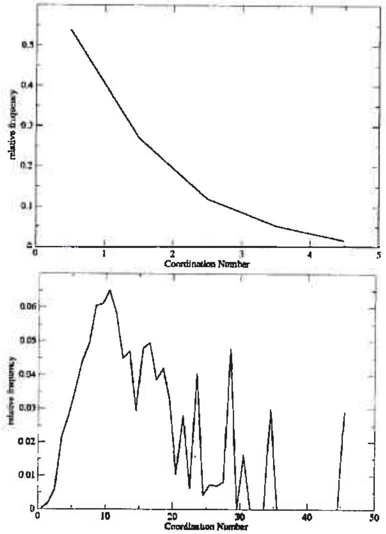

Figure 16: A coordination number plot representing the degree of connectivity within macropores (top) and micropores (bottom).

CONCLUSIONS

The combination of μCT and FIB pore scale information offers an opportunity for reservoir modelling in carbonates. The ability to cover both useful resolution and meaningful volumes in combination with the description of the connected porosity offers new input into network modelling. Being of restricted mineralogy allows a more generalised approach and it is hoped that a standardised procedure for the evaluation of key parameters such as permeability and resistivity relationships with porosity in carbonates might be developed. Ideally, this experimental approach should be seen as a potential tool to classify a specific formation, and not all carbonates generically.

ACKNOWLEDGEMENTS

Ghous acknowledges the School of Petroleum Engineering and Faculty of Engineering at UNSW for their financial Support. The authors also thank the Australian Partnership for Advanced Computing (APAC) for their support through the expertise program and APAC and the ANU Supercomputing Facility for very generous allocations of computer time. The Australian Research Council is also gratefully acknowledged for their long term support.

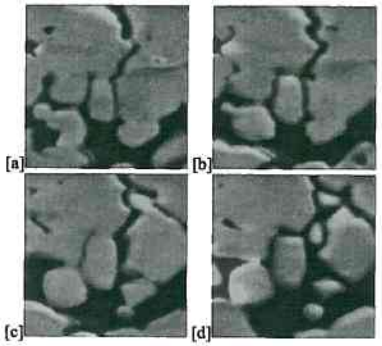

[a] [b] [c] [d]

Figure 17: An example of 2D preliminary images of 4 successive slices 200 nm apart at a resolution of 3 nanometre. Once processed into a 3D volume, structural information of grains and pores can be decorated into network models.

REFERENCES CITED

Arns, C. H., Bauget, F., Ghous, A., Sakellariou, A., Senden, T. J., Sheppard, A. P., Sok, R., Pinczewski, W. V., and Knackstedt, M. A., 2005, Digital core laboratory: Reservoir core analysis from 3D images: Petrophysics, **46**, no. 4, 260–277.

Masalmeh, S. K., and Jing, X., 2004, Carbonate scal: Characterisation of carbonate rock types for determination of saturation functions and residual oil saturations: Carbonate scal: Characterisation of carbonate rock types for determination of saturation functions and residual oil saturations:, Proceedings of the Annual Symposium of the Society of Core Analysts, SCA2004–08.

Sakellariou, A., Sawkins, T. J., Senden, T. J., Arns, C. H., Limaye, A., Sheppard, A. P., Sok, R. M., and Knackstedt, M. A., October 2003, Micro-CT facility for imaging reservoir rocks at pore scales: Micro-CT facility for imaging reservoir rocks at pore scales:, International Exposition and Seventy-Third Annual Meeting, RCT5–6:1–4.

Sheppard, A. P., Sok, R. M., and Averdunk, H., 2004, Techniques for image enhancement and segmentation of tomographic images of porous materials: Physica A, **339**, no. 1-2, 145–151.

Sheppard, A. P., Sok, R. M., and Averdunk, H., 2005, A new method for the extraction of pore networks: A new method for the extraction of pore networks:, Proceedings of the Annual Symposium of the Society of Core Analysts, SCA2005–20.

ABOUT THE AUTHORS

Abid Ghous: Abid Ghous is a doctoral candidate in Petroleum Engineering, University of New South Wales (UNSW). He has an MSc in Petroleum Engineering from UNSW (2005) and B.Sc Petroleum Engineering from University of Engineering & Technology (UET), Lahore (2002). He is working on both experimental imaging and computational analysis of microporosity and its impact on multi-phase flow and transport properties of Carbonate reservoirs. Member: SPE, SPWLA, SCA, AAPG.

Tim J. Senden: Timothy John Senden received his training and PhD in physical chemistry at the Australian National University in 1994. His principal techniques are atomic force microscopy and surface force measurement, but more recently micro-X-ray tomography. His research centres around the application of interfacial science to problems in porous media, granular materials, polymer adsorption and single molecule interactions.

Rob M. Sok: Rob Sok studied chemistry and received his PhD (1994) at the University of Groningen in the Netherlands and is currently a Research Fellow in the Department of Applied Mathematics at the Australian National University. His main areas of interest are computational chemistry and structural analysis of porous materials.

Adrian P. Sheppard: Adrian Sheppard received his B.Sc. from the University of Adelaide in 1992 and his PhD in 1996 from the Australian National University and is currently a Research Fellow in the Department of Applied Mathematics at the Australian National University. His research interests are network modelling of multiphase fluid flow in porous material, topological analysis of complex structures, and tomographic image processing.

Val W. Pinczewski: W.V Pinczewski holds BE (Chem.Eng) and PhD degrees from the University of New South Wales (UNSW). He is Head of the School of Petroleum Engineering at UNSW. His research interests include improved oil recovery, multi-phase flow and transport properties in porous media and network modelling.

Mark A. Knackstedt: Mark Knackstedt was awarded a BSc in 1985 from Columbia University and a PhD in

Chemical Engineering from Rice University in 1990. He is a Professor at and Head of the Department of Applied Mathematics at the Australian National University and a visiting Fellow at the School of Petroleum Engineering at the University of NSW. His work has focussed on the characterisation and realistic modelling of disordered materials. His primary interests lie in modelling transport, elastic and multi-phase flow properties and development of 3D tomographic image analysis for complex materials.